

Solid-spaced filters: an alternative for narrow-bandpass applications

Johan Floriot, Fabien Lemarchand, and Michel Lequime

Solid-spaced filters are composed of one or several thin wafers of excellent optical quality acting as Fabry–Perot spacer layers. We study the different steps of the design and the manufacture of filters following dense-wavelength-division-multiplexing specifications. The design method of such filters requires a tight synergy between numerical simulations and experimental characterizations to correct possible thickness errors. Experimental results of the manufacture and characterization of a three-cavity narrow-bandpass filter and of an interleaver filter are given. © 2006 Optical Society of America

OCIS codes: 060.4510, 060.1810, 230.5750, 350.2460, 310.6860.

1. Introduction

The use of the dense-wavelength-division-multiplexing (DWDM) technique has widely increased the capacity of telecommunication networks since the beginning of the 1990s, thanks to the insertion of more than 100 optical channels into 1 single-mode fiber. The spacing between adjacent DWDM channels [50 or 100 GHz in accordance with the standards defined by the International Telecommunication Union (ITU)] obviously governs the overall system performance. Specified optical characteristics of the routing components (multiplexing–demultiplexing, add–drop) include the center wavelength, the channel bandpass, the passband ripple, and the adjacent channel isolation. Thin-film interference filters (TFFs) provide efficient solutions for responding to such needs. These narrow-bandpass filters should naturally have environmental and long-term stability. They should also be easily reproducible from run to run in mass production. Hence coatings should present a dense microstructure and should require the use of energetic processes like dual-ion-beam sputtering (DIBS), ion- or plasma-source-assisted electron-beam evaporation (IAD and APS, respectively). Classical filter designs include a high

number of dielectric layers (typically more than 100) to achieve the desired bandwidth and isolation, leading to a large manufacturing time and an increase in the risk of errors during the deposition process. Moreover, the high intensity of the electric field inside the spacers magnifies the scattering losses induced by the interface roughness or the volume inhomogeneities.¹

The use of thin transparent wafers as solid spacers has been studied for various filtering applications over the last forty years.^{2–5} Solid-spaced filters (SSFs) are formed by a wafer that is in the 50–150 μm thickness range and that is coated on both sides with dielectric mirrors. The first advantage of such a structure is that the most sensitive layer of the cavity, namely the wafer, can be of excellent optical quality. The second advantage is that such filters naturally provide a narrow bandpass because of the large spacer thickness. As a result, moderate reflection factors are required for the cavity mirrors. This involves a number of coated layers that generally does not exceed seven to nine for each mirror. Moreover, a low sensitivity to deposition errors is obtained since the phase behavior of such broadband mirrors varies slowly compared with the phase shift inside the spacer layer. We proposed in recent papers,^{6,7} several DWDM designs leading to the manufacture of a double coherent solid-spaced filter.

We present in this paper more-advanced experimental results, including a three-cavity SSF following 100 GHz ITU specifications. We also give manufacturing results concerning an interleaver filter that is capable of extracting a set of 200 GHz spaced channels from a single input set of 50 GHz spaced channels.

The authors are with the Institut Fresnel, Unité Mixte de Recherche, Centre National de la Recherche Scientifique 6133, Université Paul Cézanne–Domaine Universitaire de Saint Jérôme, 13397, Marseille Cedex 20, France. F. Lemarchand's e-mail address is fabien.lemarchand@fresnel.fr.

Received 1 March 2005; accepted 13 August 2005.

0003-6935/06/071349-07\$15.00/0

© 2006 Optical Society of America

2. Design of Solid-Spaced Filters

A. Single-Cavity Filters

Let us consider a cavity sandwiched between two dielectric mirrors. Under normal illumination, the central wavelength λ_0 of the filter is given by the following equation⁸:

$$(2\pi/\lambda_0) n_{sp}d_{sp} + \delta_m = p\pi, \quad (1)$$

where p is an integer, n_{sp} and d_{sp} the refractive index and the thickness of the spacer, respectively, and δ_m the arithmetic-mean phase shift upon reflection of the two mirrors. To calculate the spectral resolution of the cavity, we introduce the geometrical mean of the reflectance of the two mirrors R_m (possibly identical in the case of SSF). The quality factor, or inverse of the resolution, is given⁸ by

$$Q = \frac{\lambda_0}{\Delta\lambda_{-3\text{ dB}}} = \left(\frac{2\pi n_{sp}d_{sp}}{\lambda_0} + \lambda_0 \frac{d\delta_m}{d\lambda} \right) \frac{\sqrt{R_m}}{(1-R_m)}. \quad (2)$$

For SSFs, the contribution of δ_m is easily controlled since we consider mirrors composed of only a few layers, which induces a smooth behavior of the phase around λ_0 . Choosing a phase value that is exactly equal to zero is not always necessary, particularly if one is interested in increasing the antireflection band of the filter. Equation (2) shows that for a given bandwidth, the lower reflectance of the mirrors can be compensated for by increasing the optical thickness of the spacer. Typically, a 17 layer mirror and a 2 μm thick spacer structure present the same quality factor as a 7 layer mirror and a 100 μm thick spacer SSF. One can note that since a SSF is naturally placed in the air on both sides, the theoretical maximum transmittance is equal to 100% for a symmetric design.

The major theoretical drawback of a SSF is that the spectral response presents many transmitted peaks with a reduced free spectral range (FSR) given by

$$\text{FSR} = \frac{\lambda_0^2}{2n_{sp}d_{sp}}. \quad (3)$$

For our applications, the FSR is typically in the 10–20 nm range. Several solutions enable us to eliminate unwanted peaks. The first one consists of using an all-dielectric blocking filter⁶ with a transmitted spectral bandwidth higher than the full width at half-maximum (FWHM) of the SSF and lower than its FSR. Of course the complexity of the whole structure increases. Other solutions consist of using multiple-SSFs.

B. Multiple-Cavity Solid-Spaced Filters

1. General Considerations

Multiple-cavity SSFs are composed of several single SSFs separated by a thin air gap in the 1–25 μm range. The air gap acts as the coupling layer of clas-

sical Fabry–Perot cavities, and the different SSFs coherently interfere. In the case of identical SSFs, the spectral response of the multiple-cavity structure presents transmittance peaks separated by the FSR given by Eq. (3). However, these peaks exhibit a spectral square shape that is typical of multiple-cavity filters. Such a design can be suitable for producing a specific grid of transmitted wavelengths (interleaver filters for instance).

On the other hand, one could be interested in obtaining a single transmittance peak. As the location of the peaks, given by Eq. (1), depends on the optical thickness of the spacer and on the phase shift of the mirrors, one solution consists of choosing cavities with different optical thicknesses. Many of the spectral coincidences will be also eliminated. This solution is discussed in Subsection 2.B.1. The second technique consists of choosing mirrors with a different phase behavior for each SSF. Equation (1) is then only satisfied for λ_0 since δ_m ($\lambda \neq \lambda_0$) is different for each SSF. Such mirrors are easy to design: For instance, let us consider a classical (HL) ^{p} quarter-wave mirror for λ_0 and a stack design (HL) ^{$p+q$} 2mH (LH) ^{q} , where p , m , and q are integers, and H and L stand for high- and low-refractive-index quarter-wave layers, respectively. The two mirrors present identical reflectance and phase for $\lambda = \lambda_0$, but as soon as $\lambda \neq \lambda_0$, the phase shifts are no longer identical.

By combining several SSFs structures with adequate spacer and mirror characteristics, we can easily extend the rejection band over the C-band.

2. Autofiltering Multiple Solid-Spaced Filters with an Optimized Transmission Window

The idea of autofiltering SSFs is to use the rejection band of a single SSF to eliminate some harmonic peaks coming from another SSF with a different cavity thickness. In this case all cavities are centered at $\lambda = \lambda_0$ but present different FSRs which provide a filtering effect over a given spectral range. The attenuation of the unwanted transmission peaks depends on the values of the different FSRs and on the mirror efficiencies. It is also possible to optimize non-quarter-wave air gaps and external layer thicknesses to eliminate ripples within the transmission window. The refinement of these thicknesses is performed with a least-square optimization procedure. Following this procedure, we give here an example of a four-cavity SSF design that fulfills the 100 GHz DWDM requirements:

- Central wavelength: $\lambda_0 = 1550$ nm.
- Transmission window: $\Delta\lambda_{0.5\text{ dB}} > 0.5$ nm.
- Spectral bandwidth: $\Delta\lambda_{-3\text{ dB}} < 0.6$ nm.
- Transmission level for a wavelength located at more than 0.5 nm of λ_0 : $T < -20$ dB.

The designed structure is composed of four silica wafers of 66, 111, 135, and 80 μm thickness (refractive index $n_{sp} = 1.44$). Each wafer has both sides coated with five-layer dielectric mirrors ($n_H = 2.1$, $n_L = 1.46$). The thickness of the fifth layer of each

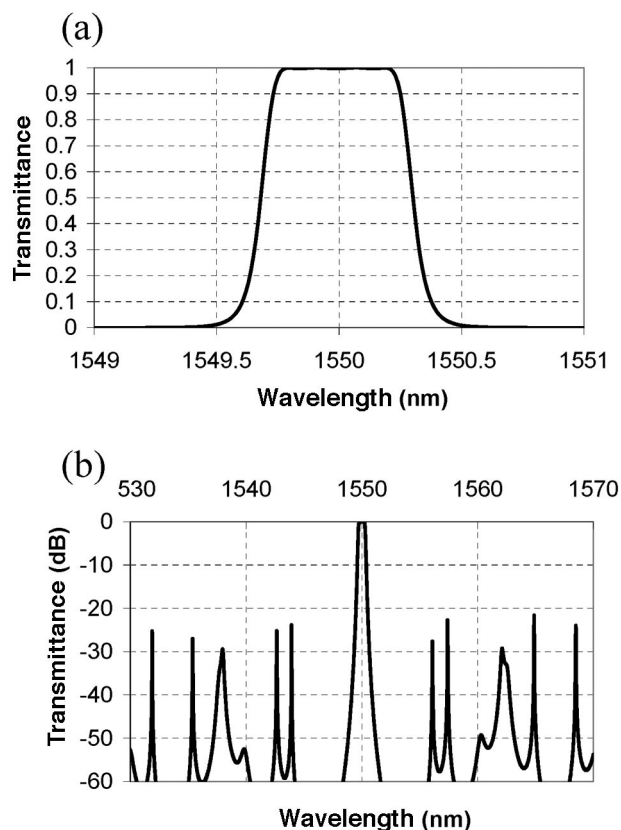


Fig. 1. Four-cavity SSF design following DWDM requirements: (a) linear scale and (b) decibel scale. The structure design is as follows: $1.09H/(LH)^2/246L_2/(HL)^2/1.05H/20.66A/$; $1.13H/(LH)^2/500L_2/(HL)^2/1.09H/24.79A/$; $1.06H/(LH)^2/412L_2/(HL)^2/1.02H/31.11A/$; and $0.73H/(LH)^2/298L_2/(HL)^2/1.27H/$, with $n_H = 2.09$, $n_L = 1.46$, $n_{L2} = 1.44$, $n_A = 1$. External medium air ($n_A = 1$).

mirror is adjusted to optimize the transmission window of the whole structure. We have plotted in Fig. 1 the spectral transmittance of this four-cavity structure with a linear scale [Fig. 1(a)] between 1549 and 1551 nm and on a decibel scale [Fig. 1(b)] over the C-band (1530–1570 nm). We stress the square shape of the achieved spectral profile, the very low insertion losses, and the efficiency of the autofiltering scheme in the C-band (residual harmonic peaks of approximately -25 dB).

3. Experimental Demonstration of an Autofiltering Three-Cavity Solid-Spaced Filter

A. Specifications and Preliminary Design

To illustrate the potential of a multiple-cavity SSF, we chose to design and manufacture a three-cavity filter centered at 1550 nm and fulfilling the 100 GHz requirements described above. The coating materials are SiO_2 (L material) and Ta_2O_5 (H material) deposited by DIBS. A preliminary design study shows that the use of three SiO_2 solid thin wafers with thicknesses of $49 \mu\text{m}$ (SSF1), $69 \mu\text{m}$ (SSF2), and $74 \mu\text{m}$ (SSF3) enables us to satisfy the specified steepness and rejection band. The specified sharpness requires the use of seven-layer mirrors. The resulting three-

SSF design is hence composed of 3 thin wafers, 42 layers, and 2 air gaps localized between the three different SSFs. Our strategy consists of first adjusting the wafer thicknesses then coating a complete mirror (seven layers) on one side of the three wafers and an incomplete mirror (six layers) on the other side, and finally adjusting the thickness of these last Ta_2O_5 layers to optimize the final performance of the filter.

B. Characterization and Adjustment of Wafer Thickness

A precise characterization of the optical thickness of each elementary wafer is mandatory. Indeed, any error concerning the geometry of a wafer (parallelism between both sides) and the value of its optical thickness at the central wavelength λ_0 of the designed filter will lead to predictable losses at the maximum level of transmittance of the final filtering device. The used wafers are commercial ones (square shaped, $10 \text{ mm} \times 10 \text{ mm}$), with a thickness-purchasing tolerance of $\pm 2 \mu\text{m}$, which does not ensure that the effective optical thickness of each cavity is an even multiple of a quarter-wavelength.

The measurement setup used to perform this accurate optical thickness characterization was already described in a previous paper⁶ and can be summed up as follows (see Fig. 2). We use a tunable laser source emitting in the C-band and an InGaAs photodiode, followed by a low-noise current amplifier to measure in one point the light power transmitted by a given wafer. The study of the variations of this transmittance level as a function of the wavelength and as a function of the position of the measurement point at the surface of this wafer enables us to determine the optical-thickness distribution corresponding to this sample. The accuracy of these optical thickness measurements is ~ 1 nm.

For our three wafers, we measure parallelism of ~ 3 arc sec, which enables us to use a Gaussian beam with a $250 \mu\text{m}$ waist without transmission losses. At the center of the wafers, the measured optical thicknesses are equal to $184.10L_2$, $258.18L_2$, and $276.26L_2$ for the SSF1, SSF2, and SSF3 wafers, respectively (L_2 is a quarter-wave layer of massive fused silica). To adjust these optical thicknesses to even values of quarter-wavelength (i.e., $186L_2$, $260L_2$, and $278L_2$), we deposit on each silica wafer a thin SiO_2 layer of appropriate thickness, then perform a new characterization of the adjusted wafers to verify that the final optical thicknesses of our three cavities (SSF1, SSF2, and SSF3) are in perfect accordance with our needs.

C. Final Design of the Filter

Simulations using the classical design-optimization method show that a square-shaped filter can be obtained by adjusting one layer of each single SSF and the two air gaps. We then simultaneously deposit a seven-layer quarter-wavelength mirror on one side of the three wafers and an incomplete six-layer quarter-wavelength mirror on the other side. The optical

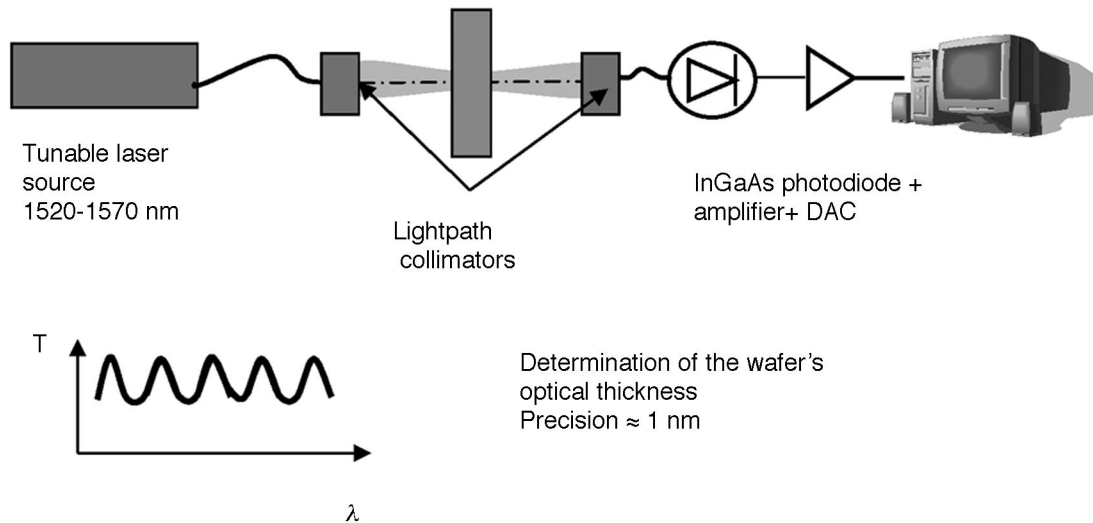


Fig. 2. Principle of measurement of wafer thickness.

monitoring of the two coatings is indirectly performed on two bare reference substrates. The analysis of the transmittance and reflectance of the two reference substrates provides an estimation of the errors performed during deposition of the two mirrors. These deposition errors are taken into account for the last design-refinement procedure. The final optimization on the two air gaps and the three remaining layers provides a set of thicknesses for the last high-index layer of the incomplete mirrors: 1.00H for SSF1 and 1.46H for SSF2 and SSF3. One can note that this design is very sensitive to errors performed on these final layers. The final design of our structure is then SSF2/air/SSF1/air/SSF3, with

$$\text{SSF1} = (\text{HL})^3\text{H}/186.01 L_2/(\text{HL})^3\text{H},$$

$$\text{SSF2} = (\text{HL})^3\text{H}/260.02 L_2/(\text{HL})^3/1.46\text{H},$$

$$\text{SSF3} = (\text{HL})^3\text{H}/278.03 L_2/(\text{HL})^3/1.46\text{H}.$$

D. Spectral Transmittance of the Three-Cavity Filter

The measured transmittance of the three single SSFs is depicted in Fig. 3. The rejection level, provided by the seven-layer mirror efficiency, is approximately -17 dB. The different locations of the harmonic peaks for SSF1, SSF2, and SSF3 should ensure an efficient autofiltering effect for the final three-cavity structure. The three transmitted peaks do not exactly coincide at 1550 nm, but the resulting effect of the coherent coupling of the three SSFs should provide the expected square-shaped profile.

The whole considered structure is SSF2/air/SSF1/air/SSF3. The relative positioning of the three elementary cavities is performed by classical mechanical means, while the fine-tuning of the air gaps is achieved by piezoelectric translators. The measured spectral transmittance of the whole filter corresponding to the optimal adjustment of these air gaps is plotted in Fig. 4.

The central wavelength is exactly 1550.0 nm, and the spectral bandwidths are equal to 0.28 nm at -0.5 dB and 0.50 nm at -3 dB [see Fig. 4(b)]. The transmittance level is below -20 dB for all wavelengths of the C-band below 1549.42 nm and above 1550.68 nm, except one sharp residual peak with a level of transmittance at approximately -15 dB [see Fig. 4(a)].

One can note that once the wafer's optical thickness is adjusted to the theoretical value, the monitoring of such filters is quite easy since only mirrors of a few layers with weak phase dispersion ($d\delta_m/d\lambda$) are required. Even in the case of deposition errors, the final centering of the different cavities is assured by correction of the mirror's final-layer thickness.

4. Experimental Demonstration of an Interleaver Filter

A. General Considerations on the Design

An interleaver device is used to simultaneously insert or extract from a network a huge number of wave-

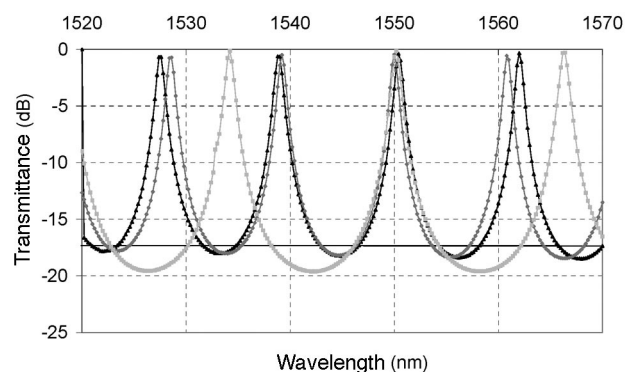


Fig. 3. Experimental transmission spectra of the three single SSFs. The structure designs are as follows: Light gray curve, $(\text{HL})^3\text{H}/186.01 L_2/(\text{HL})^3\text{H}$ (SSF1); black curve, $(\text{HL})^3\text{H}/260.02 L_2/(\text{HL})^3/1.46\text{H}$ (SSF2); gray curve, $(\text{HL})^3\text{H}/278.03 L_2/(\text{HL})^3/1.46\text{H}$ (SSF3); where H, Ta_2O_5 ; L, SiO_2 ; L_2 , silica substrate; external medium, air.

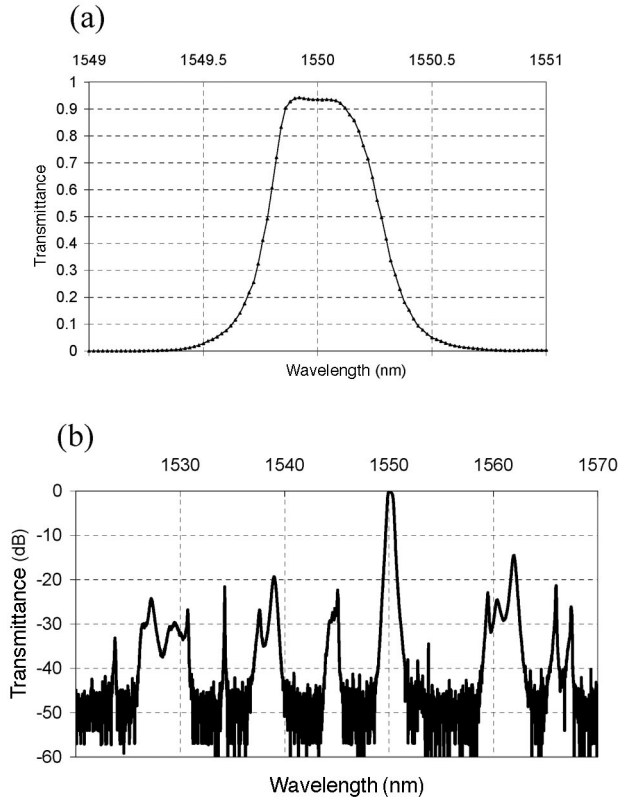


Fig. 4. Experimental transmission spectra of the three-cavity SSFs: (a) linear scale and (b) decibel scale. The structure design is as follows: SSF2/air/SSF1/air/SSF3. External medium, air.

lengths or channels. Generally, interleavers are manufactured with birefringent filters (Lyot filters), Michelson interferometers, or arrayed waveguide gratings⁹ (AWGs).

Let us consider here a 50–200 GHz interleaver filter made of three identical SSFs. In this case, the FSR of each SSF is completely defined in respect to the ITU grid. Considering a 200 GHz grid with a central frequency of 193.4 THz (i.e., a wavelength of ~ 1550 nm), the FSR should be 200 GHz or 1.603 nm. Equation (3) fixes the optical thickness of the wafers to $n_{sp}d_{sp} = 1934L_2$ at 1550 nm.

Another critical characteristic to fulfill is the rejection level of adjacent channels. It must be less than -25 dB. The width of transmission windows combined to this required rejection level defines the necessary mirror efficiency. Assuming SiO_2 (L material) and Ta_2O_5 (H material) deposited by DIBS, one should consider three-layer mirrors. Figure 5 represents the transmission spectrum of the structure on (a) a linear scale and (b) a decibel scale. It shows a 0.23 nm FWHM and a rectangular profile. The ripple amplitude is 3%. The FSR is ~ 1.6 nm, corresponding to 200 GHz as expected. Thus 1 channel among 4 are extracted, which corresponds to 31 extracted channels for the whole C-band. The theoretical rejection is -32 dB for the adjacent channels.

The last critical parameter for an interleaver filter is the transmission phase shift as a function of the

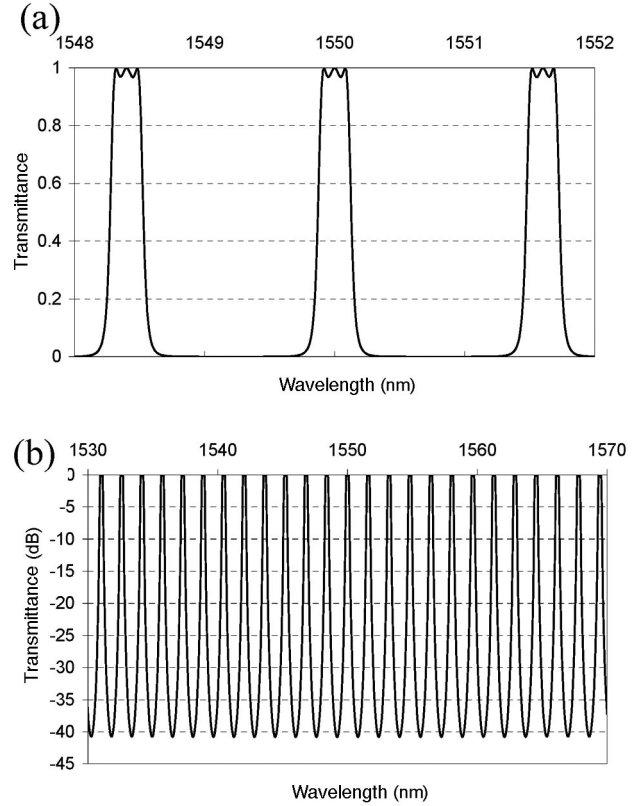


Fig. 5. Theoretical transmission spectrum of the interleaver: (a) linear scale and (b) decibel scale. The structure design is as follows: HLH/246L₂/HLH/A/, HLH/246L₂/HLH/A/, and HLH/246L₂/HLH, with $n_H = 2.09$, $n_L = 1.46$, $n_{L2} = 1.444$, $n_A = 1$. External medium air.

wavelength. The chromatic dispersion effect does indeed affect the pulse width. This effect is quantized by the study of the group-delay (GD) function defined by

$$\text{GD} = -\frac{d\Phi}{d\omega}, \quad (4)$$

where Φ is the phase of the amplitude transmission coefficient, $\omega = 2\pi c/\lambda$ is the pulsation of this light beam, and c is the speed of the light.

Figure 6 shows the theoretical variation of this GD (in picoseconds) with respect to the wavelength for the considered interleaver. The peak-to-valley variation in the transmitted window is 13 ps, which is comparable with the typical values obtained with other technologies.⁹ We note that this GD is nearly constant in a 0.2 nm bandwidth around the peak wavelength.

To manufacture such an interleaver filter, let us consider the influence of the substrate's refractive-index dispersion on the FSR value. In the case of a linear dependence of this refractive index, we obtain

$$\text{FSR}_1 = \text{FSR}_0 \left[1 + \frac{\lambda_0}{n_{sp}(\lambda_0)} \left(\frac{\partial n}{\partial \lambda} \right)_{\lambda=\lambda_0} \right], \quad (5)$$

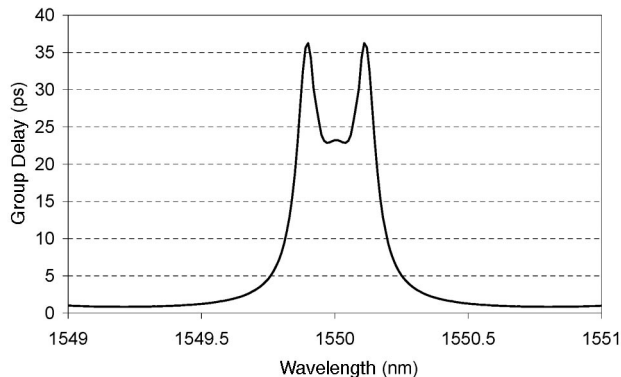


Fig. 6. Theoretical GD dispersion of the interleaver. The structure is identical to that in Fig. 5.

where FSR_0 is the free spectral range without index dispersion and FSR_1 is the new value that takes into account this index dispersion.

One can estimate the dispersion of fused silica around 1550 nm as¹⁰

$$\frac{\partial n}{\partial \lambda} (1550 \text{ nm}) = -1.2 \times 10^{-5} \text{ nm}^{-1}.$$

It ensues that the effective value of the FSR is defined by $FSR_1 = 0.987 FSR_0$. As a consequence, the optical thickness of the three silica wafers should be slightly corrected from $n_{sp}d_{sp} = 1934L_2$ to $n_{sp}d_{sp} = 1908L_2$.

B. Experimental Results

For our experimental demonstration, we selected three 500 μm thick silica substrates (purchasing tolerance of $\pm 2 \mu\text{m}$). A first characterization of these substrates was performed with the setup described in Subsection 3.B (see Fig. 2) and provides their exact optical thicknesses and parallelism (1 arc sec). Then thin silica coatings are deposited at the surface of these silica wafers to obtain the same optical thicknesses for the three elementary SSFs. To avoid the use of extremely thick coated layers, we fixed this final common value to $n_{sp}d_{sp} = 1864L_2$. This value is clearly different from the one specified by our design approach (1908 L_2), and as a consequence the transmitted peaks will not be perfectly positioned on the wavelengths defined by the ITU grid. The relative deviation between the FSR of our design and the ITU interval is equal to the relative deviation of the two design thicknesses, i.e., 2.3%.

After deposition of the three-layer mirrors, we use the same optimization procedure of the air-gap coupling as described in Subsection 3.D. Figure 7 represents the experimental transmission spectra of the optimal configuration of the SSF1/air/SSF2/air/SSF3 interleaver filter on (a) a linear scale and (b) a decibel scale. The transmission peak reaches 95%, and the FWHM of each peak is 0.23 nm. The rejection level is -27 dB for adjacent channels. The accuracy of our wavelength determination is governed by the stability of our tunable laser source, i.e., 20 pm. We

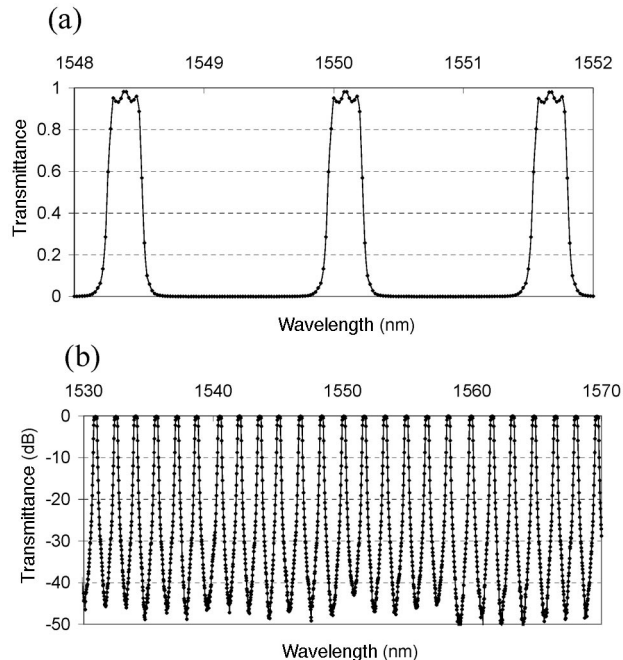


Fig. 7. Experimental transmission spectra of the interleaver: (a) linear scale and (b) decibel scale. The structure design is as follows: HLH/1864 L_2 /HLH/air; HLH/1864 L_2 /HLH/air; and HLH/1864 L_2 /HLH; where H, Ta₂O₅; L, SiO₂; L_2 , silica substrate; external medium air.

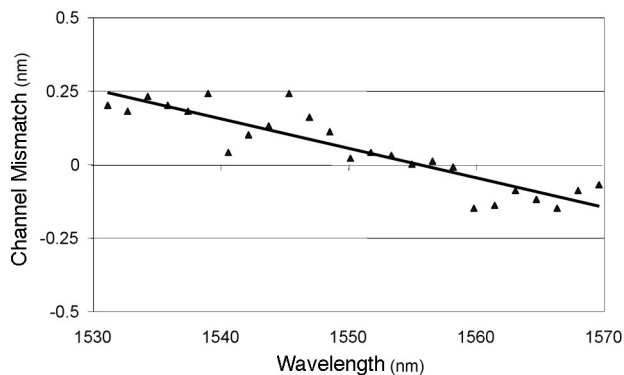


Fig. 8. Spectral mismatch between theoretical and experimental channels of the 50–200 GHz interleaver filter.

have plotted in Fig. 8 the residual mismatch between the channel wavelengths defined by the ITU grid and our experimental data. The discrepancy can be linearly approximated with a slope of approximately -16 pm/channel.

5. Conclusion

In this paper theoretical and experimental studies of multiple-cavity solid-spaced DWDM filters with and without autofiltering properties are presented. The use of non-quarter-wave layers for the mirror and the coupling layers permits us to compensate for coating-thickness errors and to strongly attenuate the ripples in the transmission window. The manufacture of a 100 GHz single-peak filter with a 95% maximum

transmission and a FWHM bandwidth of 0.5 nm is described. The measured rejection is better than -20 dB for the whole C-band. Moreover, because of the natural presence of regularly spaced transmitted peaks, SSFs are a very effective solution for the manufacture of WDM interleaver filters. The design and manufacture of a 50–200 GHz interleaver filter are presented. The maximum transmission is 95% with a 0.2 nm FWHM. The rejection reaches -27 dB for adjacent channels.

The presented experimental demonstrations of these filtering devices were achieved by using air gaps as coupling layers, but it is clear that optical contacting is the right way to assemble such filters in a compact and resistant way. The first experimental studies performed by us show that optical contacting of SSFs through dense coating layers manufactured by DIBS is perfectly feasible.¹¹ Two 100 μm thick silica wafers coated on both sides with seven-layer mirrors were assembled into a monolithic component. The resulting compact double-cavity interleaver, centered at 1550 nm, presents measured transmitted-peak maxima of $\sim 93\%$ and FWHM bandwidths of 0.5 nm. Such an assembly can provide support without unbonding thermal cycling, 100 °C thermal shocks, and mechanical stresses. Additional studies concerning the long-term stability of the component (thermal cycling and aging) should naturally be performed to ensure the viability of such filters in an industrial context.

References

1. M. Lequime, C. Deumié, and C. Amra, "Light scattering from WDM filters," in *Advances in Optical Interference Coatings*, C. Amra and A. Macleod, eds., Proc. SPIE **3738**, 268–277 (1999).
2. J. A. Dobrowolski, "Mica interference filters with transmission bands of very narrow half-widths," *J. Opt. Soc. Am.* **49**, 794–806 (1959).
3. R. R. Austin, "The use of solid etalon devices as narrowband interference filters," *Opt. Eng.* **11**, 68–69 (1972).
4. S. D. Smith and C. R. Pidgeon, "Application of multiple beam interferometric methods to the study of CO₂ emission at 15 μm ," *Mem. Soc. R. Sci. Liege Collect. 5°* **9**, 336–349 (1963).
5. A. E. Roche and A. M. Title, "Tilt tunable ultra narrow-band filters for high resolution photometry," *Appl. Opt.* **14**, 765–770 (1974).
6. J. Floriot, F. Lemarchand, and M. Lequime, "Double coherent solid-spaced filters for very narrow-bandpass filtering applications," *Opt. Commun.* **222**, 101–106 (2003).
7. J. Floriot, F. Lemarchand, and M. Lequime, "Cascaded solid-spaced filters for DWDM applications," in *Advances in Optical Thin Films*, C. Amra, N. Kaiser, and H. A. Macleod, eds., Proc. SPIE **5250**, 384–392 (2003).
8. P. W. Baumeister, *Optical Coating Technology* (SPIE, 2004).
9. S. Cao, J. Chen, J. N. Damask, C. R. Doerr, L. Guiziou, G. Harvey, Y. Hibino, H. Li, S. Suzuki, K.-Y. Wu, and P. Xie, "Interleaver technology: comparisons and applications requirements," *J. Lightwave Technol.* **LT-22**, 281–290 (2004).
10. M. Bass and E. W. Van Stryland, *Handbook of Optics*, 2nd ed. (McGraw-Hill, 1994), Vol. 1., p. 42–12.
11. J. Floriot, "Filtres bande étroite à cavités-substrats—application au domaine des télécommunications optiques", Ph.D. thesis (Université Paul Cézanne, Marseille, 2004).